Inorganic Chemistry

Article

pubs.acs.org/IC

Reactions of Superoxide with Iron Porphyrins in the Bulk and the Near-Surface Region of Ionic Liquids

Anne Dees,[†] Norbert Jux,[†] Oliver Tröppner,[†] Katharina Dürr,[†] Rainer Lippert,[†] Martin Schmid,[‡] Bernd Küstner,[§] Sebastian Schlücker,[§,∥] Hans-Peter Steinrück,[†] J. Michael Gottfried,[†,‡] and Ivana Ivanović-Burmazović*[,†]

[†]Department of Chemistry and Pharmacy, Friedrich-Alexander-Universität Erlangen-Nürnberg, Erlangen, Germany

[‡]Fachbereich Chemie, Philipps-Universität Marburg, Marburg, Germany

[§]Institute for Physical and Theoretical Chemistry, University of Würzburg, Am Hubland, 97074 Würzburg, Germany

Supporting Information

ABSTRACT: The redox reaction of superoxide (KO_2) with highly charged iron porphyrins (Fe(P4+), Fe(P8+), and Fe(P8−)) has been investigated in the ionic liquids (IL) [EMIM][Tf_2N] (1-ethyl-3-methylimidazolium bis(trifluoromethylsulfonyl)imide) and [EMIM][$B(CN)_4$] (1-ethyl-3-methylimidazolium tetracyanoborate) by using time-resolved UV/vis stopped-flow, electrochemistry, cryospray mass spectrometry, EPR, and XPS measurements. Stable KO_2 solutions in [EMIM][Tf_2N] can be prepared up to a 15 mM concentration and are characterized by a signal in EPR spectrum at $g = 2.0039$ and by the 1215 cm^{-1} stretching vibration in the resonance Raman spectrum. While the negatively charged iron porphyrin Fe(P8−) does not react with superoxide in IL, Fe(P4+) and Fe(P8+) do react in a two-step process (first a reduction of the Fe(III) to the Fe(II) form, followed by the binding of superoxide to Fe(II)). In the reaction with KO_2, Fe(P4+) and Fe(P8+) show similar rate constants (e.g., in the case of Fe(P4+): $k_1 = 18.6 \pm 0.5$ M^{-1} s^{-1} for the first reaction step, and $k_2 = 2.8 \pm 0.1$ M^{-1} s^{-1} for the second reaction step). Notably, these rate constants are four to five orders of magnitude lower in [EMIM][Tf_2N] than in conventional solvents such as DMSO. The influence of the ionic liquid is also apparent during electrochemical experiments, where the redox potentials for the corresponding Fe(III)/Fe(II) couples are much more negative in [EMIM][Tf_2N] than in DMSO. This modified redox and kinetic behavior of the positively charged iron porphyrins results from their interactions with the anions of the ionic liquid, while the nucleophilicity of the superoxide is reduced by its interactions with the cations of the ionic liquid. A negligible vapor pressure of [EMIM][$B(CN)_4$] and a sufficient enrichment of Fe(P8+) in a close proximity to the surface enabled XPS measurements as a case study for monitoring direct changes in the electronic structure of the metal centers during redox processes in solution and at liquid/solid interfaces.

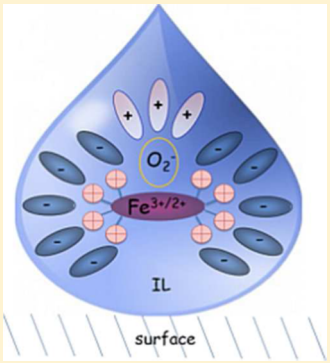

INTRODUCTION

In the vast majority of chemical reactions under aerobic conditions that are utilized for energy conversion in living organisms, ecosystems, and human society, superoxide (O_2^-, the one-electron reduction product of O_2) appears as an intermediate, which can have both beneficial and detrimental implications from biological/physiological and commercial/industrial points of view. The chemistry of superoxide is strongly related to its interactions with protons and metal centers that activate its redox transformation to oxygen and/or hydrogen peroxide (H_2O_2) within stoichiometric or catalytic processes.[1] Reactions between superoxide and metal centers are particularly relevant for the (electro)catalytic oxygen reduction and water oxidation (i.e., oxygen evolution)[2] as well as for the superoxide dismutation and superoxide reduction activity of metalloenzymes and their mimetics.[3−10]

A challenge in superoxide chemistry in solution is to find an appropriate solvent that is inert toward superoxide basicity, nucleophilicity, and redox activity, in order to obtain stable superoxide solutions of significant concentrations, suitable for reactivity and mechanistic studies.[10] In this context, the application of ionic liquids (ILs) has gained on interest, in particular for electrochemical generation of superoxide[11−18] due to the claimed stability of ILs within large electrochemical windows.[19−22] The application of ionic liquids in superoxide chemistry can offer some relevant positive aspects, especially in terms of studying reactions between superoxide and metal centers. These reactions are usually very fast, even when they proceed in a stoichiometric manner in aprotic media, and for their detailed investigations usually low temperatures are needed.[4,23] Since the majority of reactions of metal complexes are significantly slowed down in ionic liquids,[24,25] this can be valuable for their kinetic/mechanistic studies, and may enable their examination under room temperature conditions.

Another important aspect of ionic liquids is their extremely low vapor pressure, which allows for studies with ultrahigh-vacuum-based analytical techniques such as X-ray photo-

Received: April 6, 2015
Published: July 9, 2015

DOI: 10.1021/acs.inorgchem.5b00770
Inorg. Chem. 2015, 54, 6862−6872

electron spectroscopy (XPS). Recently, it has been shown that XPS can be used to study the chemical composition of ILs and their surfaces,[26−28] solutions of metal complexes in ILs,[29] and even organic reactions in ILs.[30−34] Similar studies for superoxide reactions have not been performed yet. However, for (electro)catalytic reactions with involvement of oxygen/superoxide and metal centers, the IL/solid interface can be of particular importance, due to possible and/or desired surface enrichment of the metal complexes.[29,35] Here, XPS can be a quite useful tool for the elucidation of the relevant elementary reaction steps.

To pursue the above-mentioned concept of utilizing ILs as a medium for monitoring reactions between superoxide and metal centers, we have studied the reactions of highly charged Fe(P4+), Fe(P8+), and Fe(P8−) iron porphyrins (Figure 1)

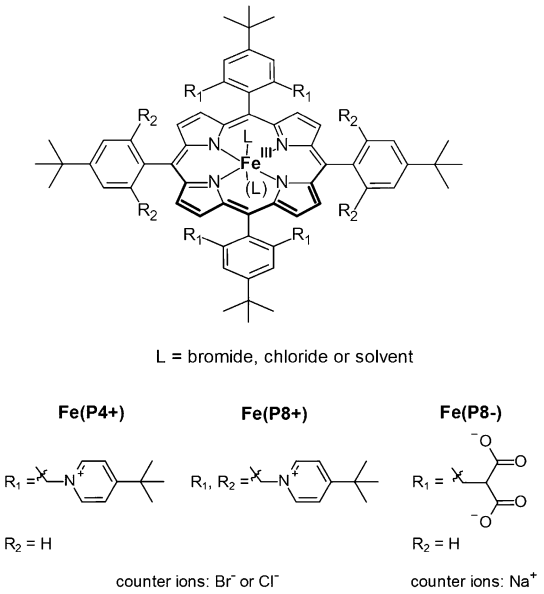

Figure 1. Porphyrins studied in this work.

with KO_2 in 1-ethyl-3-methylimidazolium bis-(trifluoromethylsulfonyl)imide, [EMIM][Tf_2N], and 1-ethyl-3-methylimidazolium tetracyanoborate, [EMIM][$B(CN)_4$], by using time-resolved UV/vis stopped-flow measurements, mass spectrometry, EPR, and XPS measurements. These complexes are known to be water-soluble,[36,37] and we found that they are soluble in ionic liquids as well. Studies of reactions of metalloporphyrins in ionic liquids are still rare.[38−44] On the other hand, iron porphyrins and their reactions with superoxide were studied in the last decades in aprotic coordinating solvents (e.g., dimethyl sulfoxide (DMSO) or acetonitrile),[4,23,45−49] where they stoichiometrically react in two steps, over the formation of iron(II) porphyrin to the iron(III)−peroxo species eqs 1 and 2.[23,48] (Some iron porphyrins are known to possess superoxide dismutating activity in aqueous solutions.[50−53]) Recently, by studying the reaction of Fe porphyrins with and without a covalently attached crown ether moiety, we have demonstrated the reversible character of the second reaction step (i.e., the reaction between the Fe(II) form of the complex and superoxide, eq 2); moreover, the nearby positive charges influence the thermodynamics, kinetics, and nature of the reaction product.[4,45] It seems that in the absence of a nearby positive charge the reaction product has predominantly the Fe(II)−superoxo character, whereas a positive charge stabilizes the iron(III)−peroxo form.[46] In general, these two redox tautomeric iron−(su)peroxo forms can coexist in an equilibrium, the position of which might be dependent on interactions with a surrounding medium.[45] By addressing these aspects as well, the herewith presented studies gain on additional, fundamental importance.

$$[Fe^{III}(porphyrin)]^+ + O_2^{\cdot -} \rightarrow [Fe^{II}(porphyrin)] + O_2 \quad (1)$$

$$[Fe^{II}(porphyrin)] + O_2^{\cdot -} \rightleftarrows [Fe^{III}(porphyrin)(O_2^{2-})]^- \quad (2)$$

EXPERIMENTAL SECTION

Materials. The majority of measurements in this study were performed using the ionic liquid [EMIM][Tf_2N], containing the 1,3-dialkylimidazolium cation, which was purchased from Merck or Iolitec with a purity of ≥99.0% and used without further purification; only for the XPS measurements [EMIM][$B(CN)_4$] was used (vide infra). The ionic liquids [EMMIM][Tf_2N], [Bu_4P][Tf_2N], [$Bu_3C_{14}H_{29}P$]Cl, and [BMPYRR][Tf_2N] were a generous gift from the group of Prof. Wasserscheid, Lehrstuhl für Chemische Reaktionstechnik, Department Chemie- and Bioingenieurwesen at the Friedrich-Alexander-Universität Erlangen. They were only used for a qualitative probing of the KO_2 solubility in the ionic liquids that do not contain the 1,3-dialkylimidazolium cations. The water content was determined using Karl Fischer titration and found to be around 30 ppm. Freshly synthesized potassium superoxide (vide infra) was used for all measurements. The ionic liquid and the superoxide powder were stored in a glovebox under argon with a water content less than 1 ppm. The same glovebox was used for all sample preparations. The synthesis of the used porphyrins H_2(P8+), Fe(P8+), and Fe(P8−) was described elsewhere.[54−56] In the case of Fe(P4+), the synthesis was performed in analogy to the known procedure for the corresponding Zn complex.[57]

Synthesis of KO_2. ^{16}O- and ^{18}O-labeled KO_2 were synthesized according to a literature procedure.[58] In a round-bottom flask (50 mL) with two nitrogen inlets and provided with a magnetic stirrer, 1.15 g of benzhydrol and 1.4 g of *t*-BuOK were added to 25 mL of dry toluene under a dry nitrogen atmosphere. One of two balloons was filled with molecular oxygen and connected with one nitrogen inlet of the flask. The second empty balloon was fixed to the second nitrogen inlet. Pressing the oxygen from one balloon into the other provided an oxygen atmosphere in the flask. The mixture was stirred for three to four hours until the color of the reaction mixture was bright yellow. The potassium superoxide was filtered under a dry nitrogen atmosphere, washed with dry toluene, and dried *in vacuo*. The already very fine powder of potassium superoxide was then transferred in an argon box to prevent hydrolyzation and pulverized in a mortar in order to enhance its solubility in ILs.

Preparation of Superoxide Solutions and Determination of Its Concentration in [EMIM][Tf_2N]. Superoxide solutions were prepared under a dry atmosphere in the argon box (H_2O < 1 ppm). The mixture of potassium superoxide powder and ionic liquid was stirred for several minutes and filtered (0.22 μm PTFE syringe filter) before measurements. The concentration of the superoxide solution in [EMIM][Tf_2N] was measured using a procedure recently published by R.-H. Liu et al.[59] In this method, superoxide reacts in two steps with the "nitro blue tetrazolium" cation (NBT^{2+}) to give formazan and diformazan, which can be followed spectroscopically. For more information see the Supporting Information.

UV/Vis Measurements. UV/vis spectra were recorded on a HP 8452A or an Analytik Jena Specord 200 spectrophotometer.

Kinetic Measurements. Kinetic data were obtained by recording time-resolved UV/vis spectra using a modified μSFM-20 Bio-Logic stopped-flow module equipped with a J&M TIDAS high-speed diode array spectrometer with combined deuterium and tungsten lamps (200−1015 nm wavelength range). Isolast O-rings were used for all sealing purposes, and solutions were delivered from 10 mL gastight

DOI: 10.1021/acs.inorgchem.5b00770
Inorg. Chem. 2015, 54, 6862−6872

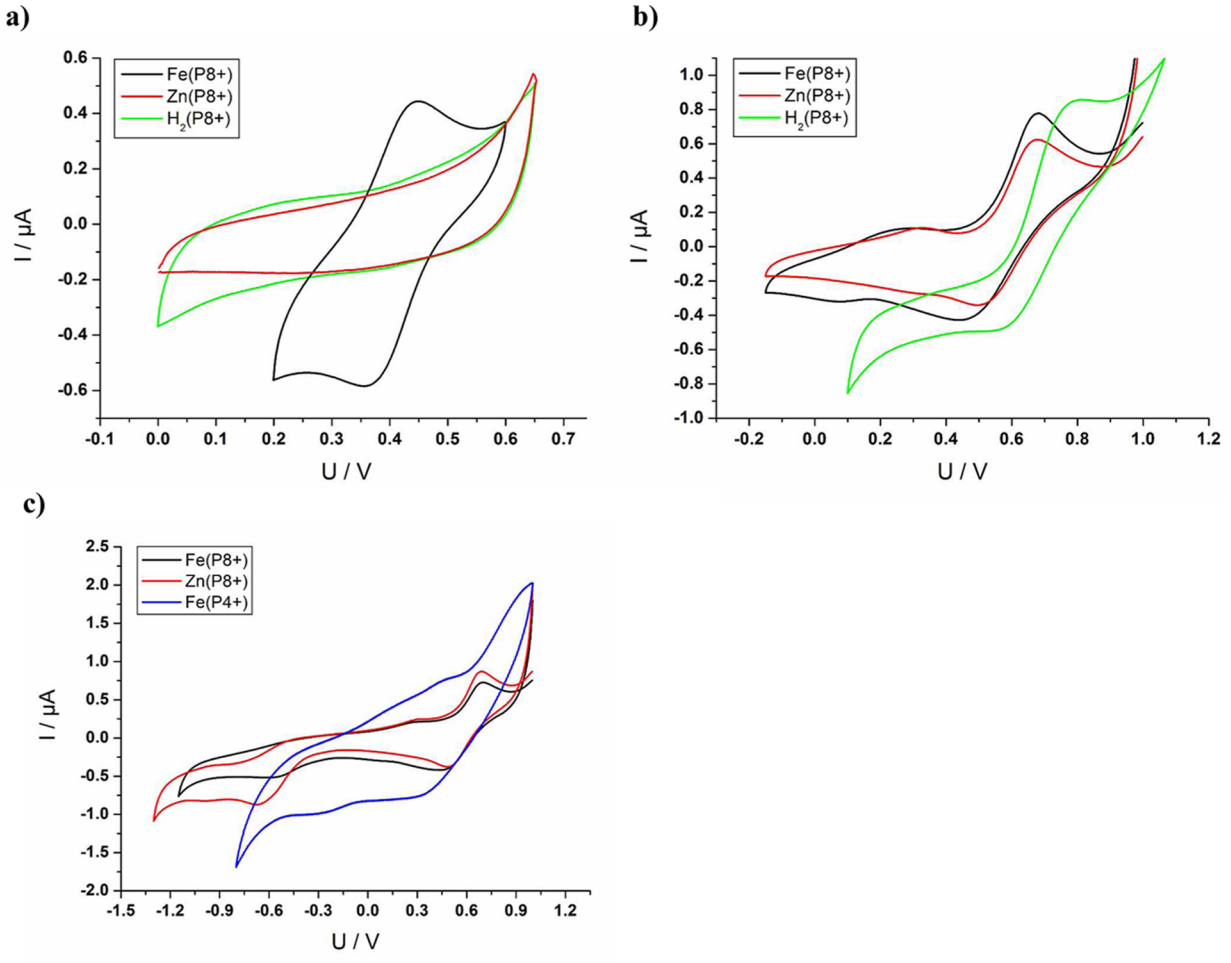

Figure 2. (a) Cyclic voltammograms of 5×10^{-4} M solutions of Fe(P8+) (black), Zn(P8+) (red), and H_2(P8+) (green) in DMSO. The potential is given vs Ag wire. The redox potential of the iron porphyrin $E_{1/2}$ is 0.28 V vs Fc/Fc^+. The scan rate was 0.01 V/s. (b) Cyclic voltammograms of 5×10^{-4} M solutions of Fe(P8+) (black), Zn(P8+) (red), and H_2(P8+) (green) in [EMIM][Tf_2N]. The potential is given vs Ag wire. The scan rate was 0.01 V/s. (c) Cyclic voltammograms of 5×10^{-4} M solutions of Fe(P8+) (black), Zn(P8+) (red), and Fe(P4+) (blue) in [EMIM][Tf_2N]. The potential is given vs Ag wire. The scan rate was 0.1 V/s.

Hamilton syringes. The syringes are controlled by separate drives, allowing for variation of the ratio of mixing volumes of superoxide and complex solutions, respectively. The observed rate constants (k_{obs}) were obtained by global analysis of the time-resolved UV/vis spectra using the Specfit/32 program. At least five kinetic runs were recorded under all conditions, and the reported rate constants (k_{obs}) represent the mean values. All measurements were done at room temperature. The concentration of complex was 5×10^{-6} M, and the concentration of freshly prepared superoxide solutions was examined as described above.

Electrochemistry. Cyclic voltammetry (CV) measurements were performed with an Autolab PGSTAT 30 device (Eco Chemie). All measurements were conducted under N_2 in a jacketed, one-compartment cell with an Au disk working electrode (geometric area: 0.07 cm^2, Metrohm), a platinum wire counter electrode (Metrohm), and a silver wire pseudo-reference electrode. The silver wire pseudo-reference electrode is commonly used in the literature for the electrochemical measurements in ionic liquids.[60] Controlled CV measurements of ferrocene were undertaken to compare the potential of the Ag wire electrode with that of a commercially available Ag/AgCl reference electrode (2 M LiCl in ethanol) for nonaqueous solutions. The potentials of the Ag wire electrode were shifted by +0.16 V and +0.05 V in comparison to the Ag/AgCl reference electrode in DMSO and [EMIM][Tf_2N], respectively (see Figure S1a in the Supporting Information).

Electrochemical reduction was performed under nitrogen at a Pt gauze working electrode with a Ag wire pseudo-reference electrode and a platinated Ti auxiliary electrode separated from the working electrode compartment by a glass frit. Potential or current was controlled with an Autolab instrument with PGSTAT 30 potentiostat. The experiment was stopped when no change in the UV/vis spectra was observed any more. Measurement of UV/vis spectra was done by use of a Hellma 661.502-QX quartz Suprasil immersion probe attached via optical cables to a 150 W Xe lamp and a multiwavelength J & M detector.

ESI Mass Spectrometry. MS measurements were performed on UHR-TOF Bruker Daltonik (Bremen, Germany) maXis, which was coupled to a Bruker cryospray unit, an ESI-ToF MS capable of resolution of at least 40,000 fwhm. Detection was in positive ion mode, and the source voltage was 4.5 kV. The flow rates were 300 μL/h. The drying gas (N_2) was held at −60 °C, and the spray gas was held at −55 °C. The machine was calibrated prior to every experiment via direct infusion of the Agilent ESI-TOF low concentration tuning mixture, which provided an m/z range of singly charged peaks up to 2700 Da in both ion modes. For the measurements without superoxide, 1×10^{-4} M porphyrin was dissolved in pure DMF or a mixture of DMF with 5×10^{-4} M [EMIM][Tf_2N] respectively. Measurements in the presence of superoxide were conducted in the mixture of DMF with 5×10^{-4} M [EMIM][Tf_2N]. An excess of solid KO_2 was added to the porphyrin solution and mixed for ten seconds prior to filtration via a 0.2 μm syringe filter and the injection into the instrument.

DOI: 10.1021/acs.inorgchem.5b00770
Inorg. Chem. 2015, 54, 6862−6872

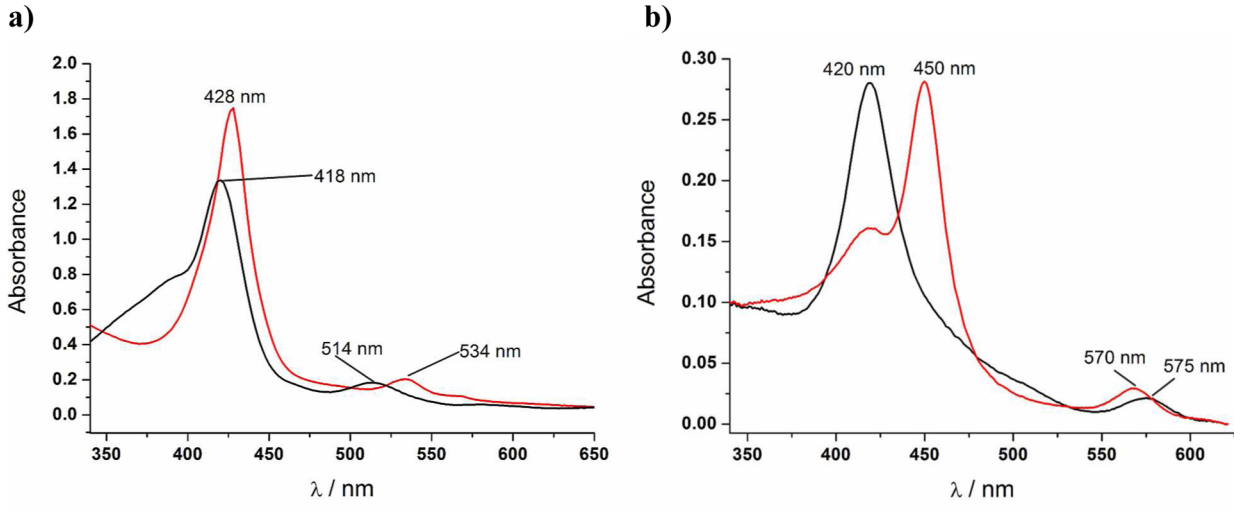

Figure 3. Electrochemical reduction of Fe^{III}(P4+) (a) and Fe^{III}(P8+) (b) in [EMIM][Tf_2N] followed by UV/vis spectroscopy. Black curves = before reduction (Fe^{III}), red curves = after reduction (Fe^{II}). The concentration of porphyrins was 5×10^{-6} M.

EPR Spectroscopy. EPR spectra were recorded on a JEOL continuous wave spectrometer JES-FA200 equipped with an X-band Gunn oscillator bridge, a cylindrical mode cavity, and a helium cryostat. A 2 mM solution of Fe^{III}(P8+) and 4 mM superoxide solution were prepared under argon and transferred in a standard quartz EPR tube. For measurement of the iron(II) porphyrin and its superoxide adduct the initial iron(III) porphyrin was reduced with ethanethiol in acetonitrile and, after removal of the organic solvents, dissolved in the appropriate amount of the ionic liquid or a freshly prepared solution of superoxide in IL, respectively.

Resonance Raman Spectra of Superoxide in [EMIM][Tf_2N]. UV resonance Raman scattering of superoxide dissolved in [EMIM][Tf_2N] was excited by the 275 nm line of an argon ion laser (Spectra Physics, Beamlok 2085). We used a custom-made rotating quartz cuvette (Hellma, Germany) to minimize photochemical degradation. The scattered light was collected at 90° and focused on the entrance slit of a double monochromator (Spex, model 1404, 85 cm focal length with 2400 grooves/mm holographic gratings). A liquid nitrogen cooled CCD (Photometrics, model SDS 9000) was used for detection. To preliminary predict the superoxide stretching vibration, DFT calculations at the B3LYP/6-311G++(3d,3p) level of theory were performed for molecules in the gas phase as well as in solution employing a polarizable continuum model (with CCl_4 as an unpolar and water as a polar solvent).

XPS Measurements. [EMIM][$B(CN)_4$] was used as ionic liquid for these measurements to avoid the oxygen and fluorine containing bis(trifluorosulfonyl)amide anion, whose XPS signals would have interfered with the signals of some of the measured species. 10 mM solutions of Fe(P8+) in [EMIM][$B(CN)_4$] were used for all measurements. For the examination of the reaction products of the iron(III) porphyrin with superoxide this solution was stirred with KO_2 powder in excess for half an hour and filtered through a syringe filter (PTFE, 0.22 μm). The XPS experiments were performed at a Scienta ESCA 200 photoelectron spectrometer, equipped with a monochromatized Al Kα X-ray source.[61] The base pressure of the UHV system was in the low 10^{-10} mbar range.

RESULTS AND DISCUSSION

Redox Behavior of Iron Porphyrins in [EMIM][Tf_2N]. Since both studied reaction steps, reduction of Fe(III) by superoxide and formation of a superoxide adduct, commonly inferred as an Fe(III)−peroxo species, eqs 1 and 2, involve an electron transfer process, it was important to get information about the redox behavior of the corresponding iron centers in the IL environment. In general, based on the known redox potentials for the O_2/O_2^- and Fe(III)/Fe(II) couples of different water- and non-water-soluble iron porphyrins,[4,53,62,63] the first reaction step can proceed via an outer-sphere electron transfer mechanism in both aqueous and aprotic solvents. Although there is no direct experimental evidence, an inner-sphere mechanism cannot be excluded.[4] However, the second reaction step, i.e., reduction of superoxide in aprotic media, can proceed only according to an inner-sphere mechanism, thus resulting in an iron−peroxo species, eq 2. To determine the redox potentials of the herein studied iron porphyrins, CV measurements were performed in DMSO and [EMIM][Tf_2N]. In case of the P8+ porphyrins, CVs were measured also for the zinc derivative Zn(P8+) and metal free porphyrin H_2(P8+), in order to get an insight into the redox processes at the porphyrin ring system in coordinated and ligand free form, respectively. By a comparison with the CVs of the iron containing porphyrins one can separate the iron-centered redox processes from those related to the porphyrin ring. In DMSO there is a reversible redox process at +0.40 V vs Ag wire for both Fe(P4+) (CV not shown) and Fe(P8+), whereas no anodic or cathodic peaks were found for Zn(P8+) and the metal free porphyrin H_2(P8+) in the same potential range (Figure 2a). Thus, this process can be ascribed to the Fe(III)/Fe(II) redox couple. Up to +0.9 V, additional oxidations have not been observed. On the other hand, Zn(P8+) in DMSO exhibits oxidation and reduction processes above +0.9 V and below −0.25 V, respectively (Figure S1c in the Supporting Information). However, in the ionic liquid there is a quasi-reversible redox process with a midpoint potential being approximately between +0.57 and +0.67 V vs Ag wire in the case of Fe(P8+), Zn(P8+), and H_2(P8+), respectively, that can be ascribed to the porphyrin ring oxidation (Figure 2b).[64] At negative voltages, starting from ca. −0.6 V vs Ag wire, a reduction process was observed for both iron complexes and the Zn complex (Figure 2c), making it difficult to unambiguously determine the iron centered Fe(III)/Fe(II) redox potential in the ionic liquid. However, bulk electrolysis monitored by UV/vis (i.e., preparative spectroelectrochemistry) showed that at least a potential of −1 V (vs Ag wire) was necessary in order to initiate the reduction of the iron centers of both Fe(P4+) and Fe(P8+) in [EMIM][Tf_2N] (Figure 3). For comparison, the reduction in DMSO could be initiated

DOI: 10.1021/acs.inorgchem.5b00770
Inorg. Chem. 2015, 54, 6862−6872

already at −0.1 V. In accordance with the electrochemical reduction, a chemical reduction of the Fe^{III}(P4+) and Fe^{III}(P8+) iron porphyrins with ethanethiol, which works instantly in organic solvents like acetonitrile and DMSO, is not successful in the ionic liquid. Consequently, the reduced Fe^{II}(P4+) and Fe^{II}(P8+) complexes are much more sensitive toward oxidation in IL than in DMSO.

These results suggest that the ionic liquid causes a shift of the metal and ring centered redox potentials of the porphyrins with a positive peripheral charge toward much lower values. This may be a consequence of strong electrostatic interactions between highly positively charged porpyrins and anions of IL that form to some extent a negatively charged solvation sphere.

For negatively charged iron porphyrins, which do not bind the negatively charged nitrite ion in conventional solvents,[56,65] there is evidence in the literature that nitrite does coordinate to the metal center in ionic liquids.[43] This observation is explained by a neutralization of the negatively charged substituents on the porphyrin ring system by cations of the ionic liquid, allowing the binding of nitrite to the iron center.[43] For the same reason, the reaction between the negatively charged superoxide and the positively charged iron porphyrin should be kinetically less favorable in ionic liquids compared to conventional solvents due to neutralization of the positively charged pyridinium substituents by anions of the ionic liquid. The negative shift of the redox potentials and our kinetic data (*vide infra*) support this hypothesis.

In addition, in the case of Fe porphyrins the anionic component of the IL can also coordinate to the metal center,[66−68] which may also explain the large negative shift of the Fe(III)/Fe(II) redox potential. It should be mentioned that the redox potential for the O_2/O_2^- couple is also negatively shifted in [EMIM][Tf_2N] (Figure S1b in the Supporting Information) compared to DMSO.[4] Thus, an outer-sphere reduction of Fe(III) by superoxide in IL is in general still feasible. Furthermore, since there is no observable difference in the electrochemical behavior between Fe^{II}(P4+) and Fe^{II}(P8+), one can conclude that the influence of the ionic liquid compensates the difference in charge. Most likely, the more positively charged iron porphyrin is surrounded by more anions of the ionic liquid, resulting in very similar redox behavior of both porphyrins.

Superoxide Solutions in [EMIM][Tf_2N]. Due to a general low stability of superoxide solutions, the effective superoxide concentration in [EMIM][Tf_2N] was measued prior to the kinetic measurements by the method described in the Experimental Section and Supporting Information. The highest concentration of KO_2 that resulted in stable superoxide solutions in [EMIM][Tf_2N] was approximately 15 mM referred to the initial weight of KO_2 was. By way of comparison, in DMSO containing tetrabutylammonium salts, quite stable 4.0 mM KO_2 solutions can be prepared.[4] However, our measurements of the superoxide concentration showed that approximately half of initially dissolved superoxide is consumed via interactions with trace amount of water as well as with the imidazolium cation (for more details see Supporting Information).[13] It should be mentioned that 1,3-dialkylimidazolium based ionic liquids containing the $[EMIM]^+$ cation are the only ones where KO_2 is soluble and gives relatively stable solutions. An attempt to dissolve a detectable amount of KO_2 in pure ionic liquids containing 1,2,3-trialkylimidazolium ([EMMIM][Tf_2N]), quaternary phosphonium ([Bu_4P][Tf_2N] and [$Bu_3C_{14}H_{29}P$]Cl) or pyrrolidinium ([BMPYRR][Tf_2N]) cations failed. It seems that the ion pairing and the formation of hydrogen bonds between the superoxide ion and the 1,3-dialkylimidazolium cation are crucial for a solvation of the hard and small superoxide anion by big and soft cations of the ionic liquid.

Superoxide solutions in [EMIM][Tf_2N] were characterized using EPR and Raman spectroscopy, as well. In the EPR spectrum (Figure 4) of KO_2 in [EMIM][Tf_2N] a strong signal

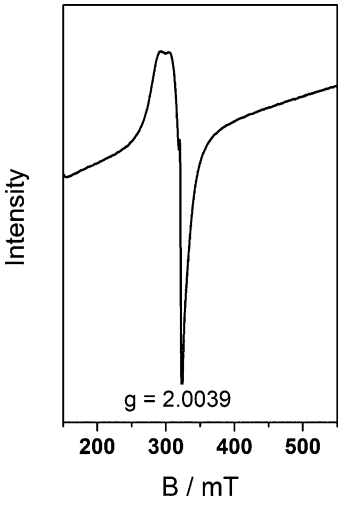

Figure 4. X-band EPR spectrum of a freshly prepared 4×10^{-3} M KO_2 solution in [EMIM][Tf_2N] measured at 8 K; microwave frequency was 8.979303 GHz, P = 1.0 mW, modulation width = 1.0 mT, sweep width 100 mT.

at g = 2.0039 can be observed (magnetic field 320.5 mT; microwave frequency of 8.98×10^9 Hz). This is close to the g value of 2.0023 for a single electron.[69] Figure 5 shows the overlay of the resonance Raman spectrum of the pure ionic liquid and of the solution of KO_2 in it, together with the corresponding difference spectrum. The peak at 1215 cm^{-1} in

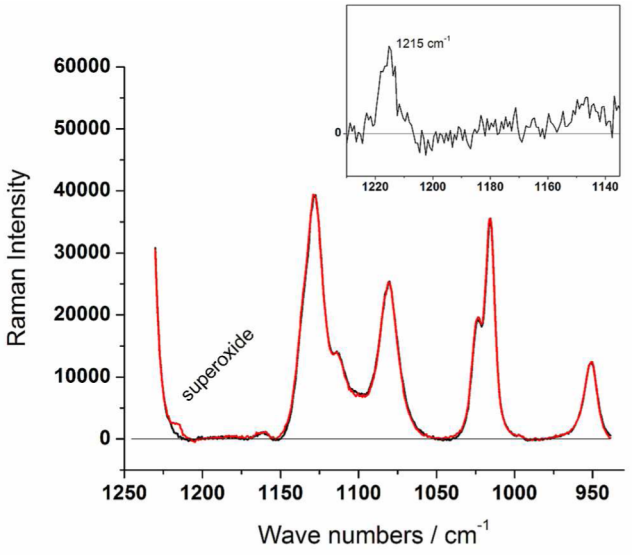

Figure 5. Resonance Raman spectra of a freshly prepared 4×10^{-3} M KO_2 solution in [EMIM][Tf_2N] (red curve) and the pure ionic liquid (black curve) measured at room temperature. Inset: Difference spectrum.

DOI: 10.1021/acs.inorgchem.5b00770
Inorg. Chem. 2015, 54, 6862−6872

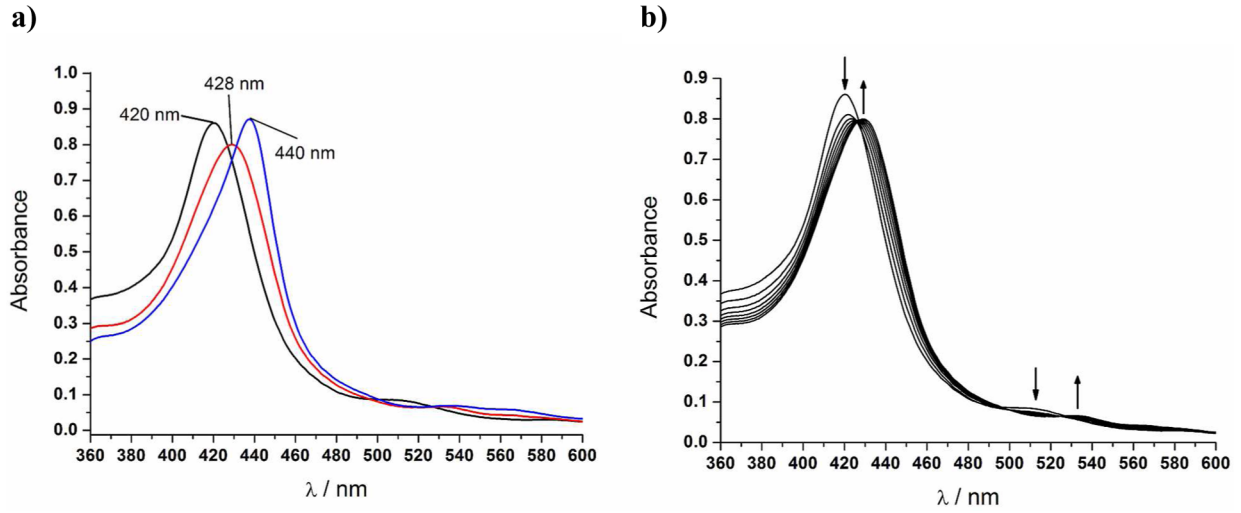

Figure 6. (a) UV/vis spectra of the reactant (black curve: [Fe^{III}(P4+)]), intermediate (red curve: [Fe^{II}(P4+)]), and product (blue curve: [Fe^{III}(P4+)(O_2^{2-})]) species along the course of the reaction between Fe^{III}(P4+) and superoxide in [EMIM][Tf_2N] at room temperature, obtained by the global spectral analysis of the corresponding time-resolved spectra. (b) Time-resolved UV/vis spectra for the first reaction step between Fe^{III}(P4+) and superoxide (the second reaction step was omitted for clarity). The concentrations of superoxide and the complex were 2×10^{-3} M and 5×10^{-6} M, respectively.

the difference UV Raman spectrum is assigned to the symmetric stretching vibration of the superoxide ion. For solid KO_2 the stretching vibration was reported to occur at 1143 or 1154 cm^{-1},[70] however, there are no reference values for solutions of KO_2 reported in the literature. Our DFT calculations (B3LYP/6311-G++(3d,3p)) indicate that a stronger solvation of superoxide (i.e., a more polar medium) shifts the symmetric stretching vibration toward higher wavenumber values. The simulation of the solvation by a continuum with the dielectric constant of water around the superoxide ion resulted in a calculated wavenumber value of 1212 cm^{-1}, which is very similar to that experimentally observed in the ionic liquid. In contrast, we obtained values of 1176 and 1186 cm^{-1} for this superoxide vibration in the gas phase and in a continuum with the dielectric constant of CCl_4, respectively. We have also performed the resonance Raman measurement of a ionic liquid solution of $K^{18}O_2$ that inevitably contains ca. 20−30% of $K^{16}O_2$.[70b] Therefore, the obtained spectrum (Figure S2 in the Supporting Information) again shows the peak at 1215 cm^{-1}, as a less intense one, which could be ascribed to the $^{16}O-^{16}O$ stretching vibration, and the main peak that is shifted to the lower frequencies and that probably could be ascribed to $^{18}O-^{18}O$ stretching vibration.

Kinetic Measurements. Prior to kinetic measurements the reactivity of the porphyrins was checked using UV/vis spectroscopy. A reaction between metal free porphyrin H_2(P8+) and superoxide could be excluded in this way (Figure S3 in the Supporting Information). The highly negatively charged porphyrin Fe(P8−) was also examined, but was found not to react with the negatively charged superoxide ion (Figure S4 in the Supporting Information), most probably due to the electrostatic repulsion and unfavorable formation of a precursor complex (required for an outer-sphere electron transfer) and/or superoxide binding (required for an inner-sphere electron transfer). Fe(P8+) and Fe(P4+) were found to react with superoxide in the ionic liquid and were thus studied by time-resolved stopped-flow kinetic measurements.

For Fe(P4+), two distinct reaction steps could be observed (Figure 6a), which were assigned to the two reaction steps given in eqs 1 and 2.[4] In the first reaction step the iron(III) porphyrin reacts with superoxide resulting in iron(II) porphyrin, followed by a second reaction step to the iron (su)peroxo adduct. Time-resolved UV/vis spectra for this reaction with the spectra of the reactant, intermediate, and product species (obtained by the global spectra analysis) are shown in Figure 6. Reduction of the iron(III) porphyrin to the iron(II) species causes a shift of the Soret and Q bands to higher wavelengths. Typical absorption bands for the Fe^{III}(P4+) occur at 418 nm (Soret band) and at 514 nm (Q-band), which are shifted to 428 nm (Soret band) and 534 nm (Q-band) in the iron(II) porphyrin, as verified by electrochemical reduction of Fe(P4+) in [EMIM][Tf_2N] (Figure 3). As it is much slower than the first reaction step, the second reaction step was observed only at higher concentrations of superoxide (≥2 mM), and the final spectrum is that of the (su)peroxo adduct with an absorption maximum at 440 nm.[4,23,45,46,48,49]

From the concentration-dependent measurements (Figure 7), the second-order rate constants for the first and the second

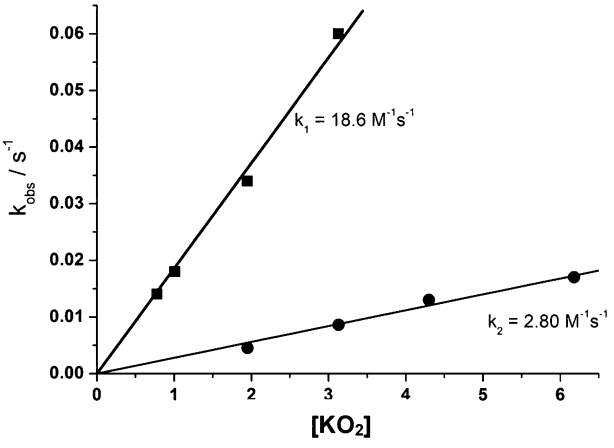

Figure 7. Plot of k_{obs} vs concentration of superoxide for the first and second reaction steps in the case of Fe^{III}(P4+).

DOI: 10.1021/acs.inorgchem.5b00770
Inorg. Chem. 2015, 54, 6862−6872

reaction steps were found to be 18.6 ± 0.5 M^{-1} s^{-1} and 2.8 ± 0.1 M^{-1} s^{-1}, respectively. Strikingly, these reaction rates are four to five orders of magnitude lower than the corresponding reaction rates for other porphyrin complexes in conventional organic solvents.[4,46] First, this could be ascribed to an extreme ionic strength effect. As the solvent exclusively consists of ions, a strong kinetic salt effect has to be considered. The iron porphyrin and the superoxide ion are of opposite charges. As a result, the rate constant for the reaction between these two ions decreases with increasing ionic strength (primary kinetic salt effect). Second, the hydrogen bonding abilities of the ionic liquid may also play a role here.[66] In the literature, the hydrogen bond donor ability, i.e., the Kamlet−Taft parameter α, is reported only for [BMIM][Tf_2N] as 0.55, where [BMIM] is 1-butyl-3-methylimidazolium.[71] As the cations are comparable, it can be assumed that the parameter α for [EMIM][Tf_2N] should be similar. In contrast, the aprotic organic solvent DMSO has an α value of zero.[71] Therefore, the imidazolium cation of the ionic liquid, in addition to electrostatic integrations, is able to build strong hydrogen bonds to solutes, especially to oxygen containing nucleophiles as it is the superoxide anion, which can affect its nucleophilicity and consequently the reaction rates. In addition, anions of the IL can coordinate to the metal center;[66−68] hence, in terms of an inner-sphere electron transfer mechanism superoxide needs to compete with the nucleophilicity of Tf_2N^- that is present in a huge excess. Also the viscosity of the ionic liquid can have a retarding effect on the reaction rate,[24,25,72,73] even though this effect is not as large as the other mentioned effects.

The reaction between KO_2 and Fe(P8+) (whose reaction with NO in water was studied in the literature)[37,56] has a more complex reaction pathway because three reaction steps were observed in the stopped-flow measurements (Figure 8 and Scheme 1). An additionally detected species was characterized to be the hydroxo complex, based on the comparison with the UV/vis spectra for the reaction between the starting Fe^{III}(P8+) and KOH in IL. Due to the unknown amount of hydroxide that is inevitably present in the KO_2 solution,[4] and its interference with the main reaction path, the kinetic parameters of a high accuracy could not be obtained for Fe(P8+). A similar behavior was previously reported by us for the iron complex of a crown ether−porphyrin conjugate in DMSO.[4] However, for the second reaction step an approximate rate constant of 1 M^{-1} s^{-1} was estimated. Similar to what was observed in electrochemical studies (*vide supra*), there is practically no difference in the reactivity of Fe(P8+) and Fe(P4+) toward superoxide considering the second reaction step eq 2.

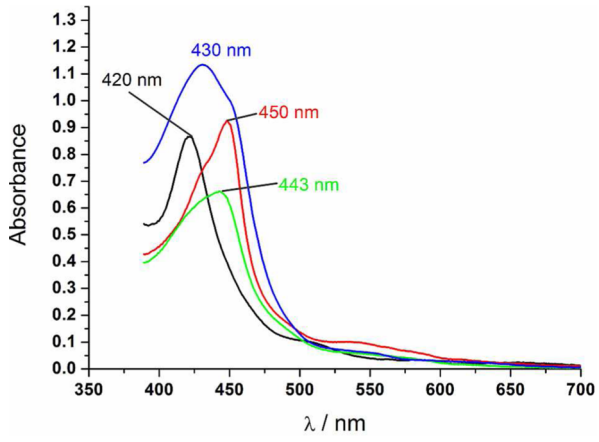

Figure 8. UV/vis spectra of the species occurring during the reaction between Fe^{III}(P8+) and superoxide in [EMIM][Tf_2N]. The curves were assigned to the following species: black curve, [Fe^{III}(P8+)]; green curve, [Fe^{III}(P8+)(OH)]; red curve, [Fe^{II}(P8+)]; blue curve, [Fe^{III}(P8+)(O_2^{2-})].

Scheme 1[a]

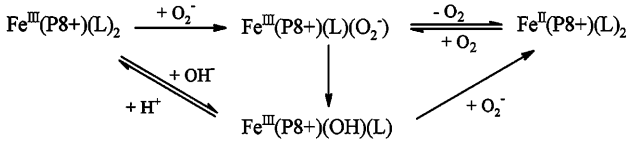

[a]L = Br^-, Cl^-, or solvent.

Mass Spectrometry. In order to characterize the products of the reaction between the positively charged iron porphyrins and superoxide, ESI mass spectrometry was performed for Fe(P4+). The measurements were performed in DMF and a mixture of ionic liquid and DMF, respectively. Since significant fragmentation of the complex was observed under the conditions of standard ESI MS measurements, cryo ultrahigh resolution mass spectrometry was performed at −60 °C. In the spectrum of the pure porphyrin in DMF, two major peaks appear at m/z = 518.9348 ($[C_{100}H_{116}FeN_8Cl_2]^{3+}$) and 817.8605 ($[C_{100}H_{116}FeN_8Cl_2Br]^{2+}$) that correspond to the intact Fe(III) complex with four positive charges on the porphyrin periphery (+5 overall charge of the complex cation) with chloride and/or bromide as either axial ligands or counteranions, respectively (Figure S5 and Table S1 in the Supporting Information). In the presence of [EMIM][Tf_2N], besides the two above-mentioned species, there is a significant peak at m/z = 918.3596 related to the Fe(III) complex with the chloride and Tf_2N^- anions (Figure 9 and Figure S6 in the Supporting Information). It seems that Tf_2N^- tends to interact with the porphyrin cation even if present only in low concentrations. One can envision that in the environment of pure [EMIM][Tf_2N] such interactions will be largely scaled up. The product mixture of the reaction between Fe(P4+) and KO_2 was also investigated in the presence of [EMIM][Tf_2N]. The resulting spectrum reveals the formation of the iron−(su)-peroxo adduct that is related to a species with the peak at m/z = 812.8858 (Figure 10).

In the mass spectra of the reaction mixture (Figure S7a in the Supporting Information) two interesting species can be observed as well, with the peaks at m/z = 500.6204 ($[C_{100}H_{116}FeN_8O)]^{3+}$, Figure S7b in the Supporting Information) and m/z = 775.4437 ($C_{100}H_{116}FeN_8(HO_2)(CH_3OH)]^{2+}$, Figure S7c in the Supporting Information). The species at m/z = 500.6204 corresponds to a formal Fe(III)−oxo adduct that might be stabilized as a (oxo)Fe(IV)($Por^{\bullet-}$)-like species, with one electron transferred to the prophyrin ring. The reduced form of the porphyrin ring could be stabilized by the high positive charge on its periphery, and a porphyrin-centered reduction process was observed by cyclic voltammetry (*vide supra*). Fe(IV)−oxo are in general known as products of the protonation of Fe(III)−peroxo species. The species at m/z = 775.4437 can be envisaged as an oxo−hydroxo-like species, i.e., oxo(hydroxo)Fe(III)- or oxo(hydroxo)Fe(IV)($Por^{\bullet-}$)-like species. (Alternatively, this species can be inferred as a reduced hydroperoxo species, i.e., Fe(I)−OOH or Fe(II)−OOH-($Por^{\bullet-}$)-like species.) Such "exotic" species probably are formed under experimental conditions of MS measurements,

DOI: 10.1021/acs.inorgchem.5b00770
Inorg. Chem. 2015, 54, 6862−6872

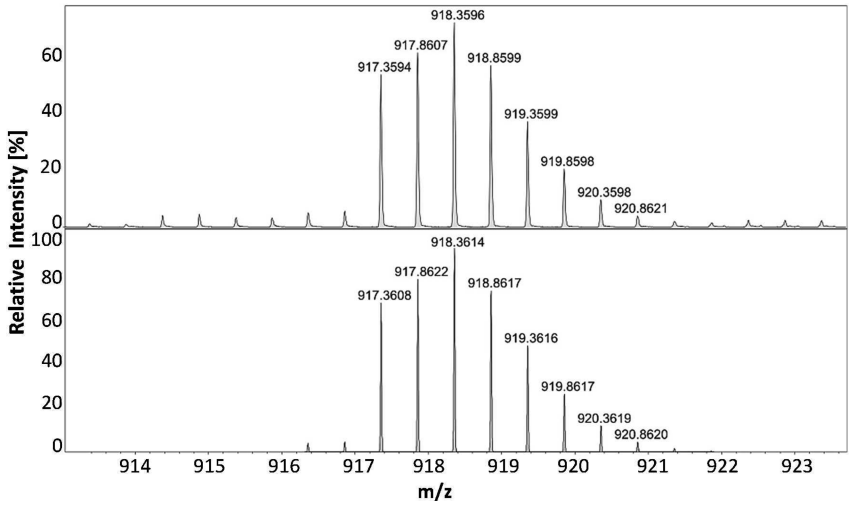

Figure 9. Cryo-UHR-ESI-ToF mass spectrum of $[C_{100}H_{116}FeN_8Cl_2(Tf_2N)]^{2+}$ (above) and simulated isotopic distribution (below) obtained for Fe^{III}(P4+) in DMF/[EMIM][Tf_2N] with a spray temperature of −60 °C and a dry gas temperature of −55 °C.

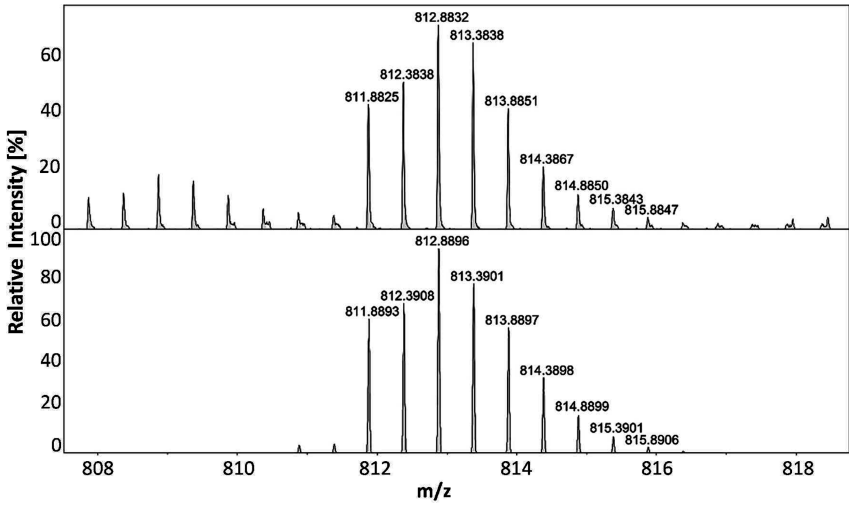

Figure 10. Cryo-UHR-ESI-ToF mass spectrum of $[C_{100}H_{116}FeN_8(O_2)(HCl)_2Cl]^{2+}$ (above) and simulated isotopic distribution (below) obtained for Fe^{III}(P4+) in DMF/[EMIM][Tf_2N] after the reaction with KO_2 with a spray temperature of −60 °C and a dry gas temperature of −55 °C.

where under high vacuum the highly positively charged porphyrin cations can easily abstract electrons and/or bind the negative (hydr)oxo ions.

EPR Spectroscopy. Pure KO_2 and three iron porphyrin samples were examined in IL: Fe^{III}(P8+), Fe^{II}(P8+) (obtained by reduction of the iron(III) porphyrin with ethanethiol), and the iron (su)peroxo species (obtained by the reaction of iron(II) porphyrin with KO_2). No signal was detected for the iron(II) complex, which is in agreement with the presence of a low-spin (S = 0) six-coordinate or an EPR silent high-spin (S = 2) five-coordinate complex. The starting material, i.e., Fe^{III}(P8+), which is a high-spin (S = 5/2) species,[55] shows an axial spectrum with $g_\perp$ = 5.71 and $g_\parallel$ = 2.02 (Figure 11a).[74] The value at g = 4.22 is related to a rhombic impurity. After reaction of the iron(II) complex with superoxide, the spectrum (Figure 11b) shows a signal for a rhombic iron(III) high-spin complex, typical for the Fe(III)−peroxo compound (g = 4.28).[45,48] The signals for superoxide are also observed ($g_\perp$ = 2.00 and $g_\parallel$ = 2.06). The $g_\parallel$ = 2.06 signal for superoxide leads to the assumption that a certain amount of bound/coordinated superoxide, in the form of Fe^{II}−superoxo complex, is present in the sample.[45] Furthermore, as the signal for the superoxide remains nearly the same after increase of temperature to 80 K, whereas the signal for free superoxide shrinks dramatically upon the same increase of temperature (Figure 12), we cannot exclude the existence of iron(II)−superoxo in an equilibrium with iron(III)−peroxo. This is in accordance with our previous studies on the superoxide adduct with the iron complex of a crown ether−porphyrin conjugate.[4,45]

X-ray Photoelectron Spectroscopy. Because of their very low vapor pressure, ionic liquids can be investigated in ultrahigh vacuum using analytical surface science techniques. For example, X-ray photoelectron spectroscopy (XPS), which is normally restricted to the analysis of solid surfaces, can be used to study the composition of ionic liquid-based solutions in the near-surface region, i.e., the topmost 6−9 nm.[75] In the literature, various studies were published examining pure ionic liquids[28,75,76] and organic reactions in ionic liquids by XPS.[31,32,77,78] Therefore, it appeared feasible to also study the redox reaction between an iron porphyrin and superoxide by XPS in ionic liquid solutions, in order to obtain complementary information on the reaction behavior. Since XPS requires a

DOI: 10.1021/acs.inorgchem.5b00770
Inorg. Chem. 2015, 54, 6862−6872

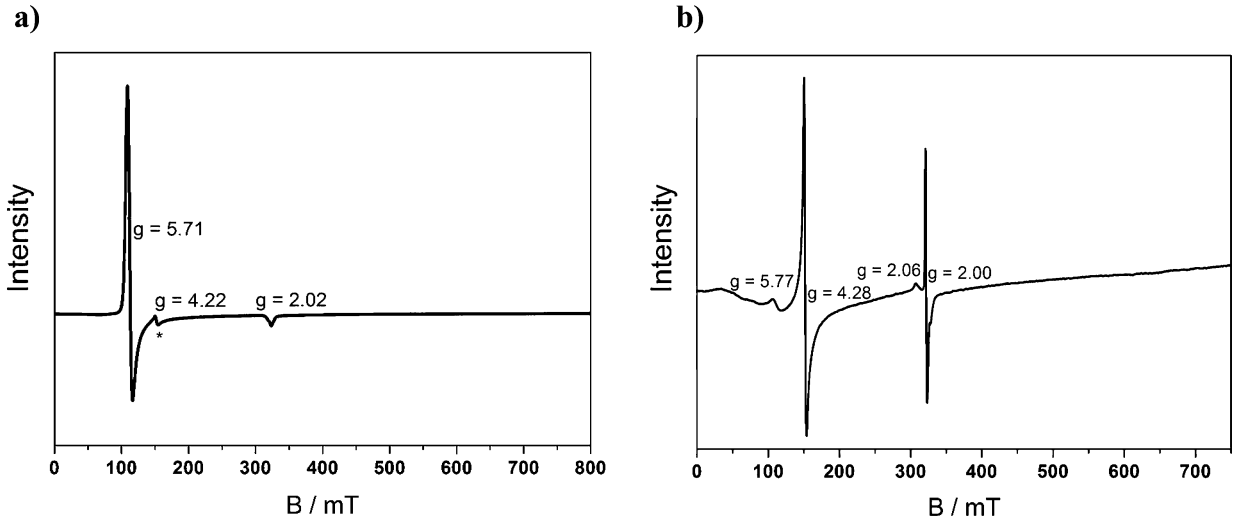

Figure 11. (a) X-band EPR spectrum of Fe^{III}(P8+) in [EMIM][Tf_2N] at 8 K; microwave frequency was 8.986141 GHz, P = 1.0 mW, modulation width = 1.0 mT, sweep width 800 mT. The signal marked with an asterisk comes from a rhombic impurity in the ionic liquid. (b) X-band EPR spectrum of Fe^{III}(P8+) with KO_2 in [EMIM][Tf_2N] at 8 K; microwave frequency was 8.984862 GHz, P = 1.0 mW, modulation width = 1.0 mT, sweep width 800 mT.

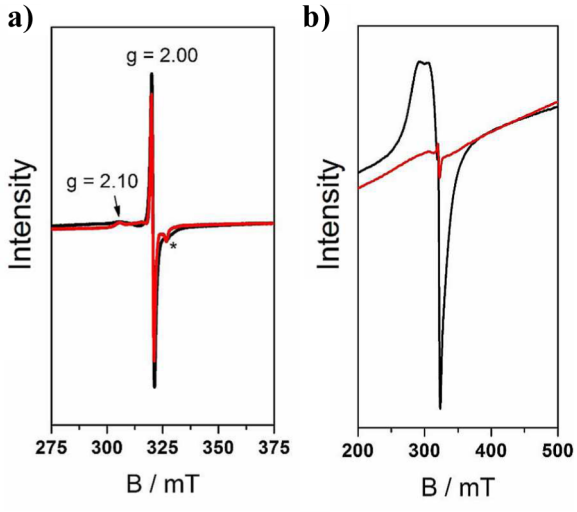

Figure 12. Temperature dependence of the superoxide signal in X-band EPR spectra. (a) Fe^{III}(P8+) with KO_2 in [EMIM][Tf_2N] at 8 K (black line) and 80 K (red line); microwave frequencies were 8.984847 GHz (at 8 K) and 8.983663 GHz (80 K), P = 1.0 mW, modulation width = 1.0 mT, sweep width 100 mT (both spectra). The signal marked with an asterisk comes from a rhombic impurity in the ionic liquid. (b) Freshly prepared 2.3 mM KO_2 solution in [EMIM][Tf_2N] measured at 8 K (black line) and 80 K (red line); microwave frequency was 8.979303 GHz, P = 1.0 mW, modulation width = 1.0 mT, sweep width 100 mT.

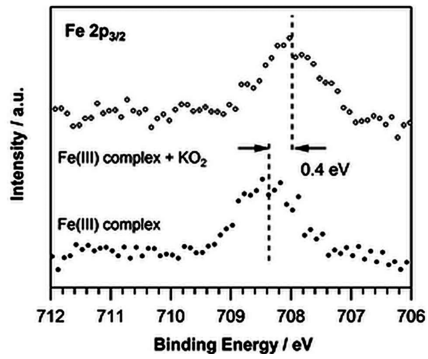

Figure 13. Fe $3p_{3/2}$ XP spectra of pure Fe^{III}(P8+) (bottom) and after reaction with KO_2 (top), in [EMIM][$B(CN)_4$].

relatively high surface concentration of the metal complexes in order to achieve a sufficient signal-to-noise ratio, Fe(P8+) porphyrin was chosen because of its higher solubility. It was found that the concentration of porphyrin in the solution has to be at least 10 mM for a successful XPS measurement. The solubility of KO_2 is in the same range of concentration. Therefore, only the first reaction step (see eq 1) can be reached by mixing the iron(III) porphyrin with superoxide, while the availability of superoxide is not sufficient for the second reaction step, the formation of the superoxo adduct. As shown in Figure 13, the first reaction step between the iron(III) porphyrin and KO_2 causes a shift of the Fe $2p_{3/2}$ signal by 0.4 eV toward lower binding energy, which is consistent with a reduction of the initial iron(III) complex to a complex in which the metal center has a reduced oxidation state, most likely an iron(II) complex.[79] This observation is in agreement with all other experimental evidence. Comparison of the Fe $2p_{3/2}$ intensities with the C 1s signals intensities related to the ionic liquid shows that the concentration of the porphyrin complexes in the near-surface region probed by XPS is approximately 10 times higher than the bulk concentration. A similar enrichment of a dissolved complex was previously observed for $[Pt(NH_3)_2]^{2+}$ in [EMIM][$EtOSO_3$], where the surface concentration exceeded the bulk concentration even by a factor of ~200.[29] Without this enrichment effect, the XPS measurement reported here would be much more difficult because of the lower signal-to-noise ratio.

CONCLUSIONS

For the first time, the reaction of the superoxide anion O_2^- with metal centers has been investigated in ionic liquids (ILs), by utilizing highly charged iron porphyrins (Fe(P4+) and Fe(P8+)). It has been demonstrated that only positively charged iron porphyrins are capable of reacting with superoxide in ILs, whereas no reaction with the negatively charged complex

DOI: 10.1021/acs.inorgchem.5b00770
Inorg. Chem. 2015, 54, 6862−6872

Fe(P8−) is detectable. This suggests that the charge on the porphyrin periphery notably affects the formation of a precursor complex between O_2^- and iron porphyrin and/or binding of superoxide to the metal center. The ionic liquids significantly influence the redox behavior of Fe(P4+) and Fe(P8+), shifting the redox potentials of the Fe(III)/Fe(II) couples by approximately 1 V toward more negative values and making the corresponding Fe(II) centers highly oxygen sensitive. In ILs, the two-step reaction with superoxide is four to five orders of magnitude slower than in conventional organic solvents and up to eight orders of magnitude slower than in aqueous solutions.[4,5] This is probably due to the extreme ion strength effect of ILs as reaction media, and due to the fact that superoxide needs to compete with the nucleophilicity of the IL anions that are in a huge excess. An interaction between the IL anion and the positively charged Fe porphyrin has been confirmed by cryo mass spectrometry. EPR and XPS measurements were employed to further characterize the reaction products. From the EPR spectra it was not possible to exclude the existence of the Fe(II)−superoxo form in equilibrium with Fe(III)−peroxo. The XPS measurements of the solution were possible due to the negligible vapor pressure of the IL and a sufficient enrichment of the Fe complex in the close proximity to the surface. Our results open new possibilities for monitoring direct changes in the electronic structure of the metal centers during redox processes in solution via XPS. The performed detection of the metal oxidation states in general, and in the case of reactions with superoxide in particular, is a valuable tool for the elucidation of the elementary reaction steps behind (electro)catalytic oxygen activation and water splitting processes in solution and (when using ultrathin IL films) also at liquid/solid interfaces. In that line, investigations of the metal-based redox catalysis are underway.

■ ASSOCIATED CONTENT

Supporting Information

Additional cyclovoltammograms, UV/vis and MS spectra, and the procedure to determine the superoxide concentration in [EMIM][Tf_2N]. The Supporting Information is available free of charge on the ACS Publications website at DOI: 10.1021/acs.inorgchem.5b00770.

■ AUTHOR INFORMATION

Corresponding Author

*Lehrstuhl für Bioanorganische Chemie der Friedrich-Alexander-Universität Erlangen-Nürnberg, Egerlandstr. 1, 91058 Erlangen, Germany. Phone: +4991318525428. E-mail: ivana.ivanovic-burmazovic@fau.de.

Present Address

‖J.M.G.: University of Duisburg-Essen, Faculty of Chemistry, Universitaetsstr. 5, 45141 Essen, Germany,

Notes

The authors declare no competing financial interest.

■ ACKNOWLEDGMENTS

A.D., I.I.-B., M.S., J.M.G., and H.-P.S. gratefully acknowledge financial support from the Deutsche Forschungsgemeinschaft through SFB 583 "Redox-active metal complexes" and through Grant Ste 620/9-1. O.T. wants to thank the "Solar Technologies Go Hybrid" initiative of the State of Bavaria.

■ REFERENCES

(1) Ivanović-Burmazović, I. *Adv. Inorg. Chem.* **2008**, *60*, 59−100.
(2) Allen, C. J.; Hwang, J.; Kautz, R.; Mukerjee, S.; Plichta, E. J.; Hendrickson, M. A.; Abraham, K. M. *J. Phys. Chem. C* **2012**, *116*, 20755−20764.
(3) Fridovich, I. *Annu. Rev. Biochem.* **1995**, *64*, 97−112.
(4) Dürr, K.; Macpherson, B. P.; Warratz, R.; Hampel, F.; Tuczek, F.; Helmreich, M.; Jux, N.; Ivanović-Burmazović, I. *J. Am. Chem. Soc.* **2007**, *129*, 4217−4228.
(5) Batinić-Haberle, I.; Rebouças, J. S.; Spasojević, I. *Antioxid. Redox Signaling* **2010**, *13*, 877−918.
(6) Aston, K.; Rath, N.; Naik, A.; Slomczynska, U.; Schall, O. F.; Riley, D. P. *Inorg. Chem.* **2001**, *40*, 1779−1789.
(7) Riley, D. P.; Schall, O. F. *Adv. Inorg. Chem.* **2006**, *59*, 233−263.
(8) Salvemini, D.; Muscoli, C.; Riley, D. P.; Cuzzocrea, S. *Pulm. Pharmacol. Ther.* **2002**, *15*, 439−447.
(9) Riley, D. P. Super-oxide dismutase mimetics. PCT Int. Appl. WO 2009/065059 A2, 2009.
(10) Ivanović-Burmazović, I.; Filipović, M. *Adv. Inorg. Chem.* **2012**, *64*, 53−95.
(11) Hayyan, M.; Mjalli, F. S.; Hashim, M. A.; AlNashef, I. M.; Tan, X. M.; Chooi, K. L. *J. Appl. Sci.* **2010**, *10*, 1176−1180.
(12) Hayyan, M.; Mjalli, F. S.; Hashim, M. A.; AlNashef, I. M.; Tan, X. M. *J. Electroanal. Chem.* **2011**, *657*, 150−157.
(13) (a) Islam, M. M.; Imase, T.; Okajima, T.; Takahashi, M.; Niikura, Y.; Kawashima, N.; Nakamura, Y.; Ohsaka, T. *J. Phys. Chem. A* **2009**, *113*, 912−916. (b) AlNashef, I. M.; Hashim, M. A.; Mjalli, F. S.; Ali, M. Q. A.-h.; Hayyan, M. *Tetrahedron Lett.* **2010**, *51*, 1976−1978. (c) Hayyan, M.; Mjalli, F. S.; Hashim, M. A.; AlNashef, I. M. *J. Mol. Liq.* **2013**, *181*, 44−50.
(14) Martiz, B.; Keyrouz, R.; Gmouh, S.; Vaultier, M.; Jouikov, V. *Chem. Commun.* **2004**, 674−675.
(15) Rogers, E. I.; Huang, X.-J.; Dickinson, E. J. F.; Hardacre, C.; Compton, R. G. *J. Phys. Chem. C* **2009**, *113*, 17811−17823.
(16) Katayama, Y.; Onodera, H.; Yamagata, M.; Miura, T. *J. Electrochem. Soc.* **2004**, *151*, A59−A63.
(17) Katayama, Y.; Sekiguchi, K.; Yamagata, M.; Miura, T. *J. Electrochem. Soc.* **2005**, *152*, E247−E250.
(18) Sethupathy, P. K.; Monnier, J. R.; Matthews, M. A.; Weidner, J. W. *Anal. Bioanal. Electrochem.* **2013**, *5*, 711−718.
(19) Hapiot, P.; Lagrost, C. *Chem. Rev.* **2008**, *108*, 2238−64.
(20) Bonhote, P.; Dias, A. P.; Papageorgiou, N.; Kalyanasundaram, K.; Gratzel, M. *Inorg. Chem.* **1996**, *35*, 1168−1178.
(21) Buzzeo, M. C.; Klymenko, O. V.; Wadhawan, J. D.; Hardacre, C.; Seddon, K. R.; Compton, R. G. *J. Phys. Chem. A* **2003**, *107*, 8872−8878.
(22) Korotcenkov, G. Ionic Liquids in Gas Sensors. In *Handbook of Gas Sensor Materials*; Springer: New York, 2014; Vol. 2.
(23) McCandlish, E.; Miksztal, A. R.; Nappa, M.; Sprenger, A. Q.; Valentine, J. S.; Stong, J. D.; Spiro, T. G. *J. Am. Chem. Soc.* **1980**, *102*, 4268−4271.
(24) Weber, C. F.; Puchta, R.; van Eikema Hommes, N. J. R.; Wasserscheid, P.; van Eldik, R. *Angew. Chem., Int. Ed.* **2005**, *44*, 6033−6038.
(25) Begel, S.; Illner, P.; Kern, S.; Puchta, R.; van Eldik, R. *Inorg. Chem.* **2008**, *47*, 7121−7132.
(26) Gottfried, J. M.; Maier, F.; Rossa, J.; Gerhard, D.; Schulz, P. S.; Wasserscheid, P.; Steinrück, H. P. *Z. Phys. Chem.* **2006**, *220*, 1439−1453.
(27) Steinrück, H.-P. *Surf. Sci.* **2010**, *604*, 481−484.
(28) Smith, E. F.; Villar Garcia, I. J.; Briggs, D.; Licence, P. *Chem. Commun.* **2005**, 5633−5635.
(29) Maier, F.; Gottfried, J. M.; Rossa, J.; Gerhard, D.; Schulz, P. S.; Schwieger, W.; Wasserscheid, P.; Steinrück, H.-P. *Angew. Chem., Int. Ed.* **2006**, *45*, 7778−7780.
(30) Kolbeck, C.; Niedermaier, I.; Taccardi, N.; Schulz, P. S.; Maier, F.; Wasserscheid, P.; Steinrück, H.-P. *Angew. Chem.* **2012**, *124*, 2664−2667.

DOI: 10.1021/acs.inorgchem.5b00770
Inorg. Chem. 2015, 54, 6862−6872

(31) Niedermaier, I.; Kolbeck, C.; Taccardi, N.; Schulz, P. S.; Li, J.; Drewello, T.; Wasserscheid, P.; Steinrück, H.-P.; Maier, F. *ChemPhysChem* **2012**, *13*, 1725−1735.
(32) Steinruck, H.-P. *Phys. Chem. Chem. Phys.* **2012**, *14*, 5010−5029.
(33) Niedermaier, I.; Taccardi, N.; Wasserscheid, P.; Maier, F.; Steinrück, H.-P. *Angew. Chem., Int. Ed.* **2013**, *52*, 8904−8907.
(34) Niedermaier, I.; Bahlmann, M.; Papp, C.; Kolbeck, C.; Wei, W.; Krick Calderón, S.; Grabau, M.; Schulz, P. S.; Wasserscheid, P.; Steinrück, H.-P.; Maier, F. *J. Am. Chem. Soc.* **2014**, *136*, 436−441.
(35) Kolbeck, C.; Paape, N.; Cremer, T.; Schulz, P. S.; Maier, F.; Steinrück, H.-P.; Wasserscheid, P. *Chem. - Eur. J.* **2010**, *16*, 12083−12087.
(36) Jee, J. E.; Eigler, S.; Hampel, F.; Jux, N.; Wolak, M.; Zahl, A.; Stochel, G.; van Eldik, R. *Inorg. Chem.* **2005**, *44*, 7717−7731.
(37) Jee, J. E.; Wolak, M.; Balbinot, D.; Jux, N.; Zahl, A.; van Eldik, R. *Inorg. Chem.* **2006**, *45*, 1326−1337.
(38) Srinivas, K. A.; Kumar, A.; Chauhan, S. M. S. *Chem. Commun.* **2002**, 2456−2457.
(39) Chatel, G.; Goux-Henry, C.; Mirabaud, A.; Rossi, T.; Kardos, N.; Andrioletti, B.; Draye, M. *J. Catal.* **2012**, *291*, 127−132.
(40) Kumari, P.; Sinha, N.; Chauhan, P.; M. S. Chauhan, S. *Curr. Org. Synth.* **2011**, *8*, 393−437.
(41) Zhang, H.-J.; Liu, Y.; Lu, Y.; He, X.-S.; Wang, X.; Ding, X. *J. Mol. Catal. A: Chem.* **2008**, *287*, 80−86.
(42) Li, Z.; Xia, C.-G.; Xu, C.-Z. *Tetrahedron Lett.* **2003**, *44*, 9229−9232.
(43) Schmeisser, M.; van Eldik, R. *Inorg. Chem.* **2009**, *48*, 7466−7475.
(44) Wan, Q.-X.; Liu, Y. *Catal. Lett.* **2009**, *128*, 487−492.
(45) Duerr, K.; Olah, J.; Davydov, R.; Kleimann, M.; Li, J.; Lang, N.; Puchta, R.; Hubner, E.; Drewello, T.; Harvey, J. N.; Jux, N.; Ivanovic-Burmazovic, I. *Dalton Trans.* **2010**, *39*, 2049−2056.
(46) Duerr, K.; Troeppner, O.; Olah, J.; Li, J.; Zahl, A.; Drewello, T.; Jux, N.; Harvey, J. N.; Ivanovic-Burmazovic, I. *Dalton Trans.* **2012**, *41*, 546−557.
(47) Dürr, K.; Jux, N.; Zahl, A.; van Eldik, R.; Ivanović-Burmazović, I. *Inorg. Chem.* **2010**, *49*, 11254−11260.
(48) Burstyn, J. N.; Roe, J. A.; Miksztal, A. R.; Shaevitz, B. A.; Lang, G.; Valentine, J. S. *J. Am. Chem. Soc.* **1988**, *110*, 1382−1388.
(49) Selke, M.; Sisemore, M. F.; Valentine, J. S. *J. Am. Chem. Soc.* **1996**, *118*, 2008−2012.
(50) Ilan, Y.; Rabani, J.; Fridovich, I.; Pasternack, R. F. *Inorg. Nucl. Chem. Lett.* **1981**, *17*, 93−96.
(51) Kasugai, N.; Murase, T.; Ohse, T.; Nagaoka, S.; Kawakami, H.; Kubota, S. *J. Inorg. Biochem.* **2002**, *91*, 349−355.
(52) Batinic-Haberle, I.; Spasojevic, I.; Hambright, P.; Benov, L.; Crumbliss, A. L.; Fridovich, I. *Inorg. Chem.* **1999**, *38*, 4011−4022.
(53) Aitken, J. B.; Shearer, E. L.; Giles, N. M.; Lai, B.; Vogt, S.; Reboucas, J. S.; Batinic-Haberle, I.; Lay, P. A.; Giles, G. I. *Inorg. Chem.* **2013**, *52*, 4121−4123.
(54) Jux, N. *Org. Lett.* **2000**, *2*, 2129−2132.
(55) Guldi, D. M.; Rahman, G. M. A.; Jux, N.; Balbinot, D.; Hartnagel, U.; Tagmatarchis, N.; Prato, M. *J. Am. Chem. Soc.* **2005**, *127*, 9830−9838.
(56) Jee, J. E.; van Eldik, R. *Inorg. Chem.* **2006**, *45*, 6523−6534.
(57) Sarova, G. H.; Hartnagel, U.; Balbinot, D.; Sali, S.; Jux, N.; Hirsch, A.; Guldi, D. M. *Chem. - Eur. J.* **2008**, *14*, 3137−3145.
(58) Rosenthal, I. *J. Labelled Compd. Radiopharm.* **1976**, *12*, 317−318.
(59) Liu, R.-h.; Fu, S.-y.; Zhan, H.-y.; Lucia, L. A. *Ind. Eng. Chem. Res.* **2009**, *48*, 9331−9334.
(60) (a) Khoshtariya, D. E.; Dolidze, T. D.; van Eldik, R. *Chem. - Eur. J.* **2009**, *15*, 5254−5262. (b) Dolidze, T. D.; Khoshtariya, D. E.; Illner, P.; Kulisiewicz, L.; Delgado, A.; van Eldik, R. *J. Phys. Chem. B* **2008**, *112*, 3085−3100.
(61) Lukasczyk, T.; Flechtner, K.; Merte, L. R.; Jux, N.; Maier, F.; Gottfried, J. M.; Steinrück, H.-P. *J. Phys. Chem. C* **2007**, *111*, 3090−3098.
(62) Su, Y. O.; Kuwana, T.; Chen, S.-M. *J. Electroanal. Chem. Interfacial Electrochem.* **1990**, *288*, 177−195.
(63) Rana, M. S.; Tamagake, K. *J. Electroanal. Chem.* **2005**, *581*, 145−152.
(64) Wolak, M.; van Eldik, R. *Chem. - Eur. J.* **2007**, *13*, 4873−4883.
(65) Jee, J. E.; Eigler, S.; Jux, N.; Zahl, A.; van Eldik, R. *Inorg. Chem.* **2007**, *46*, 3336−3352.
(66) Illner, P.; Begel, S.; Kern, S.; Puchta, R.; van Eldik, R. *Inorg. Chem.* **2009**, *48*, 588−597.
(67) Illner, P.; Puchta, R.; Heinemann, F. W.; van Eldik, R. *Dalton Trans.* **2009**, 2795−2801.
(68) Hubbard, C. D.; Illner, P.; van Eldik, R. *Chem. Soc. Rev.* **2011**, *40*, 272−290.
(69) Odom, B.; Hanneke, D.; D'Urso, B.; Gabrielse, G. *Phys. Rev. Lett.* **2006**, *97*, 030801.
(70) (a) Hunter-Saphir, S. A.; Creighton, J. A. *J. Raman Spectrosc.* **1998**, *29*, 417−419. (b) Yamamoto, H.; Mashino, T.; Nagano, T.; Hirobe, M. *Tetrahedron Lett.* **1989**, *30*, 4133−4136.
(71) Lungwitz, R.; Friedrich, M.; Linert, W.; Spange, S. *New J. Chem.* **2008**, *32*, 1493−1499.
(72) Illner, P.; Kern, S.; Begel, S.; van Eldik, R. *Chem. Commun.* **2007**, 4803−4805.
(73) Kern, S.; Illner, P.; Begel, S.; van Eldik, R. *Eur. J. Inorg. Chem.* **2010**, *2010*, 4658−4666.
(74) Chaudhary, A.; Patra, R.; Rath, S. P. *Indian J. Chem., Sect. A* **2011**, *50A*, 432−437.
(75) Cremer, T.; Kolbeck, C.; Lovelock, K. R. J.; Paape, N.; Wölfel, R.; Schulz, P. S.; Wasserscheid, P.; Weber, H.; Thar, J.; Kirchner, B.; Maier, F.; Steinrück, H.-P. *Chem. - Eur. J.* **2010**, *16*, 9018−9033.
(76) Kolbeck, C.; Killian, M.; Maier, F.; Paape, N.; Wasserscheid, P.; Steinrück, H.-P. *Langmuir* **2008**, *24*, 9500−9507.
(77) Kolbeck, C.; Niedermaier, I.; Taccardi, N.; Schulz, P. S.; Maier, F.; Wasserscheid, P.; Steinrück, H.-P. *Angew. Chem., Int. Ed.* **2012**, *51*, 2610−2613.
(78) Steinrück, H. P.; Libuda, J.; Wasserscheid, P.; Cremer, T.; Kolbeck, C.; Laurin, M.; Maier, F.; Sobota, M.; Schulz, P. S.; Stark, M. *Adv. Mater.* **2011**, *23*, 2571−2587.
(79) Moulder, J. F.; Stickle, W. F.; Sobol, P. E.; Bomben, K. D. *Handbook of X-ray Photoelectron Spectroscopy*; Perkin-Elmer Corporation, Physical Electronics Division: Eden Prairie, MN, 1992.

DOI: 10.1021/acs.inorgchem.5b00770
Inorg. Chem. 2015, 54, 6862−6872